

## **ANALYSIS OF THERMAL AND MECHANICAL BEHAVIOR OF COPPER MOULD DURING THIN SLAB CASTING**

Joong Kil Park<sup>\*</sup>, Indira V. Samarasekera<sup>\*</sup>,  
Brian G. Thomas<sup>\*\*</sup>, U\_Sok Yoon<sup>\*\*\*</sup>

\* University of British Columbia, Vancouver, BC  
Canada

\*\* University of Illinois, Urbana, IL, USA

\*\*\* POSCO, Kwangyang, Korea

### **ABSTRACT**

Three-dimensional finite-element thermal-stress models have been developed to predict temperature, distortion and residual stress in the mould of thin slab continuous casters. Geometrically, there are two kinds of mould to achieve high-speed casting: funnel-shaped and parallel mould. The mould shape and high casting speed leads to higher mould temperatures and shorter mould life than in conventional slab casters. The purpose of this study is to investigate the heat flux and the effects of mould shape on distortion of the mould in a thin slab caster. Mould wall temperature measured in the plant was analyzed to determine corresponding the heat-flux profiles in thin slab moulds using an Inverse Heat Conduction model, and this data was then used in an elastic-visco-plastic analysis to investigate the deformation of the moulds in service for different the mould shapes. The model predictions of temperature and distortion during operation match plant observations. During operation, the hot face temperature reaches 430°C and the copper plates bend toward the steel, with a maximum outward distortion of about 0.3mm. This occurs just above the center of the wide faces, and

is smaller than the distortion of a conventional slab mould.

Key Word: Thin slab, mould distortion, heat flux, finite element, mathematical model

### **1. INTRODUCTION**

One of the more important recent trends in the steel industry has been the focus on the development of processes for casting steel closer to the final product size. The advanced continuous casting process for thin slabs with thickness of only a few centimeters allows hot direct rolling to be performed in-line with a few conventional finishing mill, eliminating the need for a roughing train and the associated capital costs.

The speed of the process is still limited below the five-fold increases expected and several quality problems prohibit the casting of crack sensitive grades with this process. The role of mold heat transfer and distortion in these problems has received relatively little attention in previous literature.

The mould is the most critical component of the thin slab caster, because, during casting, the copper mould plates control initial solidification of the steel product, which determines surface quality. During operation, although mould distortion due to the steep thermal gradient is small, it affects the size of gap between the solidified shell and the mould, which in turn controls heat transfer. The accompanying thermal stress may cause permanent creep deformation near the meniscus, which affects mould life as well. Therefore, maintaining a reliable, crack-free mould within close dimensional tolerances is also

crucial to safety and productivity. The issue of thermal distortion in continuous casting moulds has been discussed in the literature over the past years [1-3].

This work was undertaken to provide insight into thin slab mould behaviour using three-dimensional (3-D) finite-element models of heat transfer and stress of thin slab moulds of different configuration.

## 2. HEAT FLUX PROFILES IN THE PARALLEL MOULD BASED ON THE PLANT TRIAL

### 2.1 Measurement of mould temperature

Some relevant details of the thin slab casting mould for the measurement of mould temperature are summarized in Table 1. The plant trial was conducted for a parallel mould with a section size of 1260mmx70mm cast at a nominal speed of 3.6m/min. The mould was Cu-Cr-Zr with dimensions given by Table 1. In this table, effective wall thickness is defined as minimum distance from water in the channels to the hot face. The total mould length was 1000mm. Thermocouples were embedded through holes drilled in the bolts to a depth of approximately 22mm from the hot face.

Fig.1 shows the average temperature profiles corresponding to a time of 5 minutes into casting, along the length of mould. As shown in this figure, all the temperatures on the loose face are higher than those of the fixed face by 20-30°C, especially near the meniscus. The reasons for these differences are not known and need to be elucidated in a future study.

Table 1 Details of thin slab casting mould for measurement of mould temperature in this study

Mould length (mm)	1000
Mould coppers	Cr-Zr
Slab thickness (mm)	70
Effective wall thickness (mm)	
- broad face	25
- narrow face	22
Meniscus level (mm)	100
Nominal cooling water section (mm x mm)	5x10
No. of channels on broad faces	136
Cooling water velocity (m/s)	10.7
Water flow rate (l/min.)	
- broad face	4330
- narrow face	3600
Casting speed (m/min)	~ 3.5-4

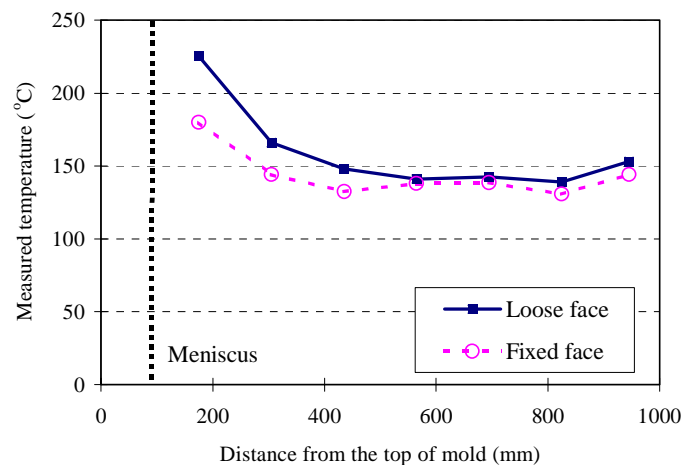


Fig.1 Time-averaged profiles of parallel mould temperature

## 2.2 Heat flux profiles

In order to calculate the heat flux profile down the mould wall, the Inverse Heat Conduction Program (IHCP) was used, which has recently been developed at UBC [5]. The solution of the IHCP is effected by minimizing the least square error between the measured temperatures and those computed by direct solution, using the estimated value of the heat flux components. The problems of uniqueness and stability, inherent in the solution of such an ill-posed problem can be solved by the use of a “regularization” technique [5]. The calculated axial profiles of the mould hot-face heat flux are shown in Fig.2. Heat flux profiles show the same tendency as measured temperature profiles. At the position of 175mm from the top of the mould, heat flux at the loose face is about  $5\text{MW/m}^2$ , while that of fixed face is about  $4\text{MW/m}^2$ . These heat fluxes are considerable higher than values reported for conventional slab casting.

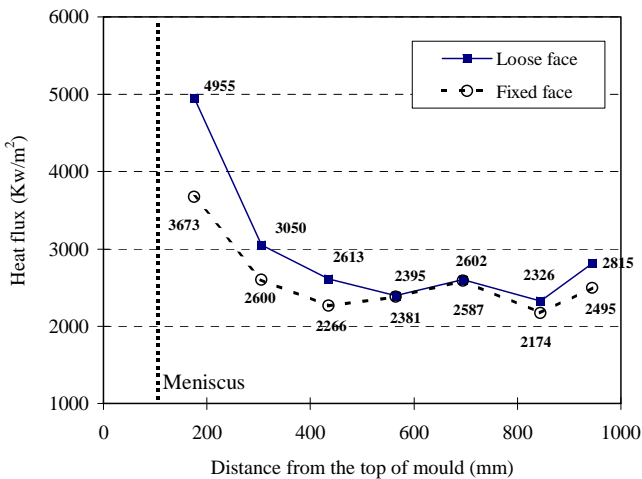


Fig.2 Heat flux profiles down the mould wall

An attempt has been made to fit heat-flux profiles as a function of the residence time of the strand in the mould. There are many popular

forms of empirical equations for heat-flux profile [6-12]. Among them, a function of the following type was selected for fitting the heat-flux profile:

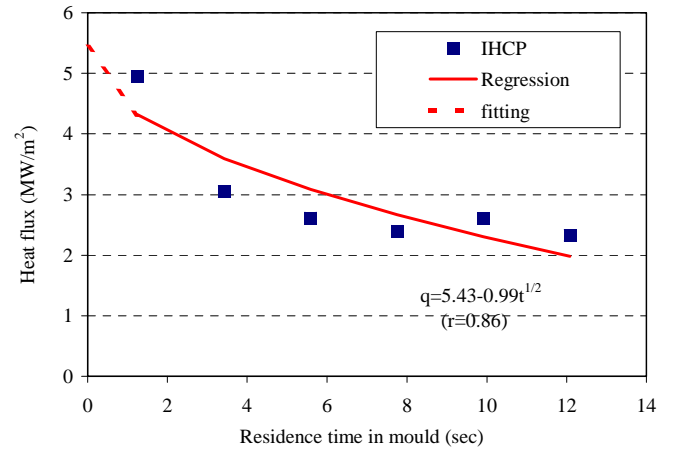
$$q = a - b\sqrt{t} \quad (1)$$

Here,  $q$  is the heat flux ( $\text{KW/m}^2$ ) down the mould length,  $t$  is the residence time (second) of the strand below the meniscus.

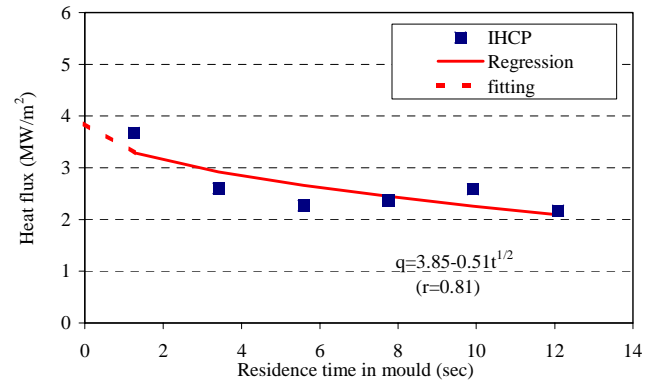
When analyzed using the least square regression method employed in the IHCP calculation, the following results were obtained (see Fig.3 (a), (b)):

$$q = 5403 - 990\sqrt{t} \quad (\text{for loose face}) \quad (2)$$

$$q = 3856 - 506\sqrt{t} \quad (\text{for fixed face}) \quad (3)$$



(a) Loose face of mould



(b) Fixed face of mould

Fig.3 Axial heat flux profiles with respect to the residence time in mould

### 2.3 Verification of heat flux equation

In order to validate the above equation, the total heat fluxes have been calculated from the water  $\Delta T$  method (energy balance) for each face of the mould. During the process of cooling the mould, the water itself heats up, and this temperature differential ( $\Delta T$ ) between the inlet and outlet could be used to monitor heat removal by the mould. Multiplying the temperature rise for each face with the corresponding water flow rate gives us the total rate of heat removal from that face. Dividing this by the exposed mould face area gives an average value for the heat extracted by that face. Ideally, this value should be equal to the heat fluxes obtained when equation (2), (3) are integrated over the residence time of the strand in the mould. Considering the variation of measured temperature, as can be seen from Fig.3, the selected function is a good approximation of the heat flux variation down the mould length.

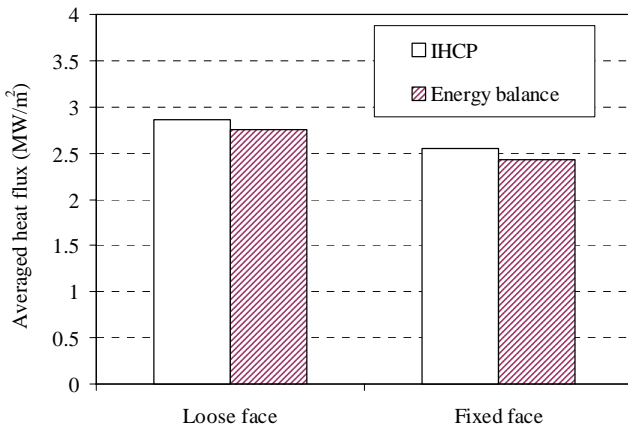


Fig.4 Comparison of average heat-flux calculated from fitted heat flux equation (IHCP) and energy balance

## 3. MODEL DESCRIPTION

Finite-element models were developed to calculate temperature, the corresponding distorted

shape in parallel and funnel moulds during steady operating conditions and after cooling to ambient temperature using the commercial stress-analysis package, ABAQUS 5.8[13]. Model domains include typical two-dimensional (2-D) horizontal sections through the copper plates, a 3-D model of a representative vertical segment of the mould, and a complete 3-D model of one-quarter section of the mould, including the water jackets and bolts. Simulation conditions for the 3-D model of a quarter of the mould are given in Table 2.

Table 2 Simulation conditions in this work

#### a) Material properties

item	Copper (plate)	Steel(Bolt)
Conductivity (W/mK)	350	49
Density (Kg/m <sup>3</sup> )	8940	7860
Elastic modulus (GPa)	130	200
Thermal expansion Coeff. (1/K)	11.7x10 <sup>-6</sup>	17.7x10 <sup>-6</sup>
Poisson ratio	0.34	0.3

#### b) Operation condition

Slab width (mm)	1260	
Casting speed(m/min.)	3.6	
Water slot heat transfer Coeff. (W/m <sup>2</sup> K)	38.45 (wide), 36.17(narrow)	
Meniscus level	100mm	
Heat flux (KW/m <sup>2</sup> )	Loose side	5430-993*t <sup>1/2</sup>
	Fixed side	3856-505*t <sup>1/2</sup>
Cooling water temperature (°C)	Inlet	37.8
	Outlet	48.1

### c) Mould geometry

		Parallel mould	Funnel mould
Slab thickness (mm)		1260	
Mold height (mm)		1000	
Cu plate thickness (mm)		60 (wide), 70 (narrow)	80 (wide), 70 (narrow)
Water slot depth (mm)		35	35 - 55
Bolt diameter (mm)		16	16
Distance between bolts(mm)		188	
Clamping force (kN)	Top (0.58m from bottom)	19	
	Bottom (0.1m from bottom)	44	
Tension bolt force	Tightening torque, N-m	120	
	Friction coefficient	0.2 – 0.6	

### 3.1 Heat Flow Model

Heat flux data was input to the exposed surfaces of copper elements on the mould hot faces as a function of distance down the mould based on previous studies.

The water-slot heat transfer coefficient  $h$ , of  $38 \text{ kWm}^{-2}\text{K}^{-1}$  is determined from the following dimensionless correlation [14].

$$\frac{h_1 D}{k_w} = 0.023 \left( \frac{D \mu_w \rho_w}{\mu_w} \right)^{0.8} \left( \frac{C_p \mu_w}{k_w} \right)^{0.4} \quad (4)$$

Where,  $D$  is hydraulic diameter of slot,  $k_w$  is thermal conductivity,  $\mu_w$  is viscosity,  $\rho_w$  is density,  $C_{pw}$  is specific heat of cooling water.

The 3-D segment model domain, shown in Figure 5, reproduces the complete geometric

features of a typical region (Fig.5 a) through the copper wide face discretized into a fine mesh. To simplify the geometry for the 3-D quarter-mould model, a pseudo-model was created using a course mesh. The temperature field produced by the pseudo-model was arranged to match that of the 3-D segment model by increasing the heat transfer coefficient artificially. The accuracy of this approach was validated using the refined 3-D model of a representative slice.

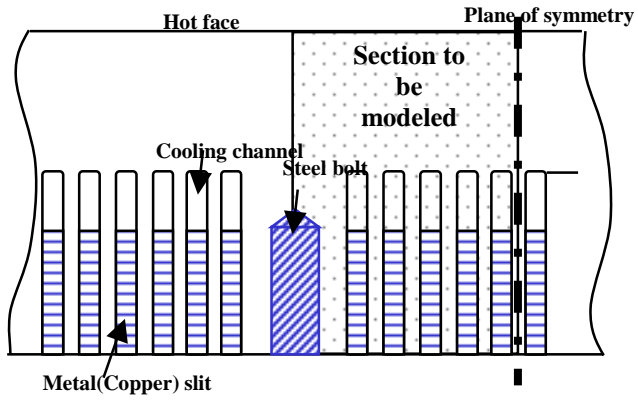
### 3.2 Stress Model

Fig.6 shows the top view of the 3-D model of a quarter section of the mould examined to analyze mould deformation. The 3-D quarter-mould model includes separate domains for the mould coppers and water jackets which are coupled mathematically only at those points where they connect mechanically in the caster during operation. The cold side of the copper wide face is mathematically bolted to the back of the water jacket at 40 locations using two-node bar elements. Boundary conditions include clamping forces on the exterior of the water jacket and pre-tension of 44kN on each bolt. The interface elements were used to model the surface element between the wide and narrow faces of the mould, the mould and water jacket, assuming small relative sliding between them in order to avoid penetrating into each other when they are deformed. And, rigid body motion is prevented by constraining the symmetry planes from normal expansion and by fixing a single point.

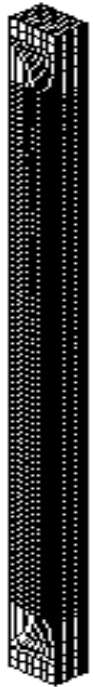
This elastic-plastic-creep stress model assumed isotropic hardening with a temperature-dependent yield stress function, shown in Figure 7. Considering that total time of operation is within 100Hrs, primary creep is taken into account by the following equation [1].

$$\dot{\epsilon}(s^{-1}) = 2.48 \times 10^{14} \exp\left(\frac{-197,000}{8.31T(K)}\right) [\sigma(ksi) - 23.]^3 [t(s)]^{-0.92}$$

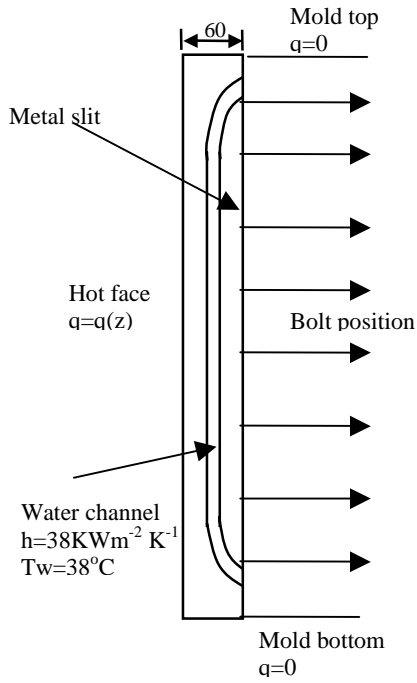
----- (5)



(a)



(b)



(c)

Fig.5 2-D horizontal section through wide face showing detailed model domain(a) and corresponding 3-D section mesh(b) and it's boundary conditions(c)

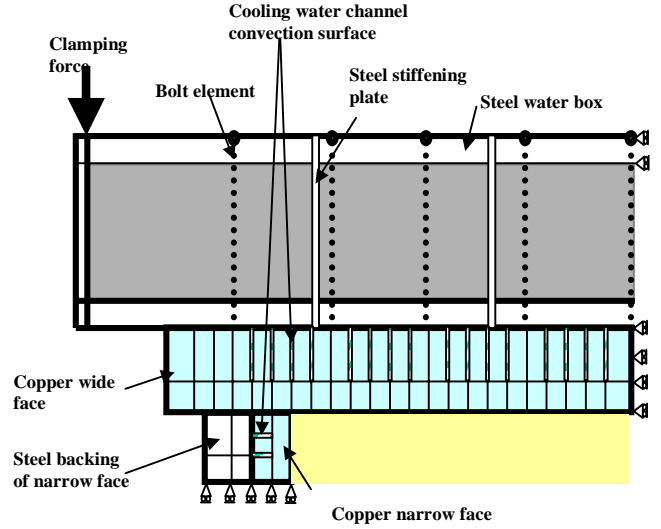


Fig.6 Top view of 3-D quarter mould model showing boundary conditions

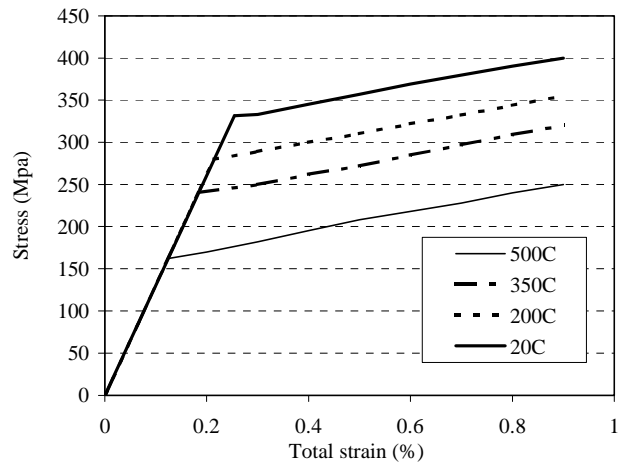


Fig. 7 Stress strain curves for copper(Cr-Zr alloy) used in model[1]

## 4. MODEL VALIDATION

### 4.1 Temperature

Fig.8 shows the temperature profiles at the location of the thermocouples along the mould length for the wide faces of the mould based on the 3-D model of a representative vertical segment of the mould. The wiggles are caused by extra angled water slots added to cool the region near the meniscus except for near to the bolt holes containing the thermocouples. As can be seen from this figure, although there is some difference between measured and calculated values, on the whole, the model predictions were found to be in a good agreement with measured temperature except at the position of 175mm from the top of mould. The latter discrepancy is due to the use of fitted a heat flux value at the meniscus, and an inverse model which neglects axial heat conduction and some geometric details such as bolt and extra angled water slot. This comparison confirms that the heat flux curves in Fig. 3 are reasonable except for a possible under-prediction of heat flux near the meniscus.

### 4.2 Distortion during operation

Fig.9 shows a comparison of measured and predicted distortion of wide and narrow faces along the line of intersection for the parallel mould. With regard to the measured values, the gap at the junction of the wide and narrow face was measured by using a gap sensor.

Although the calculated value is larger than the measured value, this model gives a reasonably accurate prediction of mould behavior. The gap between the plates above the meniscus may cause serious problems, since mould flux could penetrate, freeze, and aggravate mould wear at this critical junction [1].

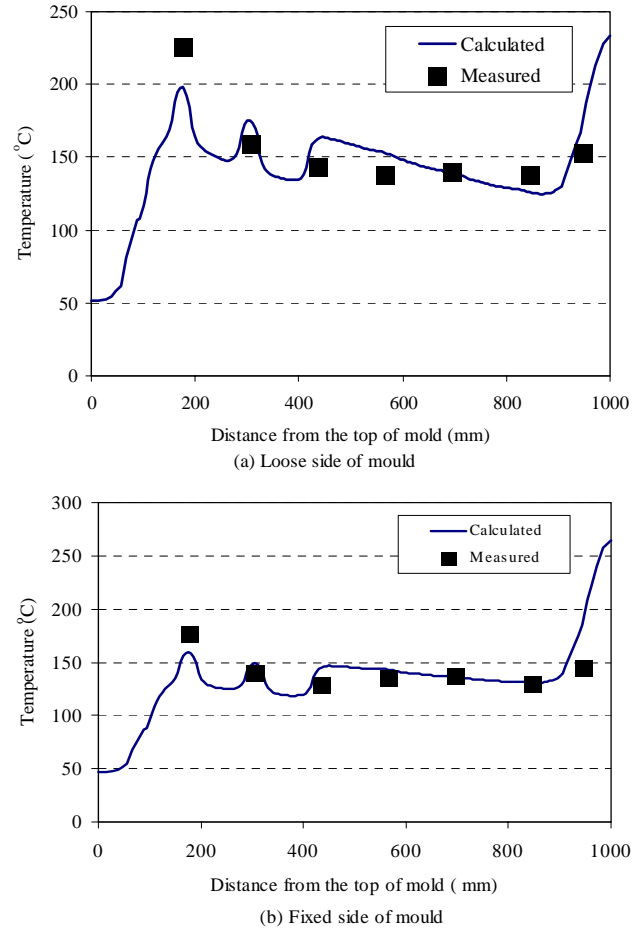


Fig.8 Comparison of temperature profile between the measured and calculated ones for the parallel mold

Fig.10 shows a comparison of the distortion of the backing plate with the measured data from a conventional casting mould. With regard to the measured data, only a few conventional slab mould distortion measurements have been performed during operation [16-18]. In addition, the distortion is influenced greatly by the casting speed, mould construction, and slab width and so on. Therefore, it is difficult to make a direct comparison. However, the predicted trend shown in Figure 10 appears to be comparable to measurements.

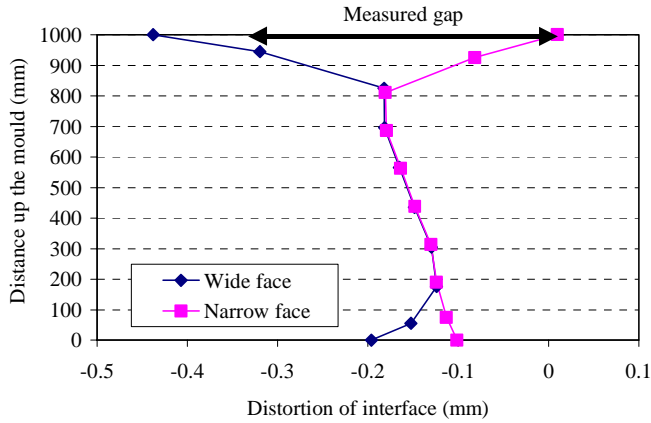


Fig.9 Distortion of wide and narrow face along the line where they meet in the mold for parallel mould

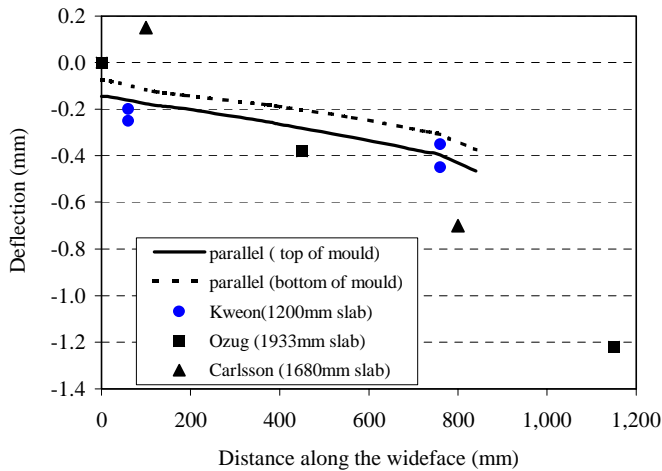


Fig.10 The behavior of bak plate distortion during operation

## 5. THERMAL AND MECHANICAL BEHAVIOR OF THIN SLAB MOULD

### 5.1 Temperature profiles of hot face

Fig.11 shows the temperature distribution of the hot face along the mould length for a parallel mould. As can be seen from Fig.11, the

maximum temperature of the wide face is approximately  $430^{\circ}\text{C}$ , which is below the softening temperature of Cu-Cr-Zr copper ( $500^{\circ}\text{C}$ ) [18]. It is important to note that within about the 50mm of the mould exit, the model predicts an increase in hot-face temperature of  $150^{\circ}\text{C}$ , which is expected to be hot, due to lack of a channel at the end of the water slot 28mm above mould exit. This is the same location where Salkiewicz et. al. [3] measured a two to sevenfold increase in wear.

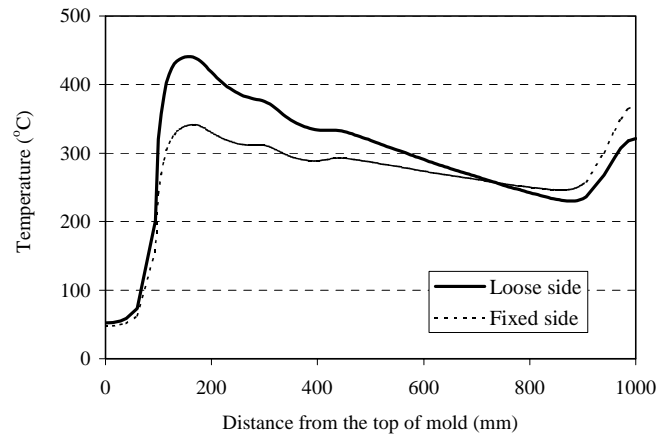


Fig.11 Hot face temperature distribution along the mold length for the parallel mold

### 5.2 Mould distortion behavior

The typical temperature and distorted shape of the parallel quarter mould during operation are shown in Figures 12-13 for conditions in Table 2. Figure 12 shows the mesh, temperature contours on the hot face, and the distorted shape of the mould, exaggerated fifty-fold. At the hot face, the maximum temperature is found to occur approximately 20mm below the meniscus.

The results shown in Figures 12-13 provide insight into the mechanical behavior of the mould during operation. The copper hot face expands in proportion to its temperature increase, but is



restrained by the cold copper beneath it. Consequently, the copper plates bend outward toward the molten steel in a manner similar to the conventional slab mould [1]. The peak distortion of 0.3mm, which occurs below the meniscus along the center of the wide face, is smaller than that of conventional caster predicted by Thomas [1], although the heat flux is higher for thin slab casting.

The bending of the copper plates stretches the bolts and pulls away from the front of the water jacket during operation. Although there is bolt pre-stress of 44kN, a thin gap forms just below the meniscus, as shown in Figure 13. The gap in a 60mm parallel mould is about 0.2mm where distortion is greatest.

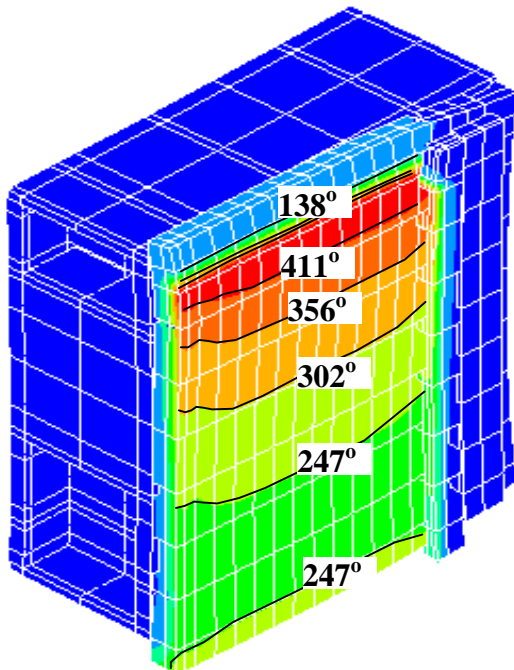


Fig.12 Temperature contours on distorted mould shape during operation for parallel mold

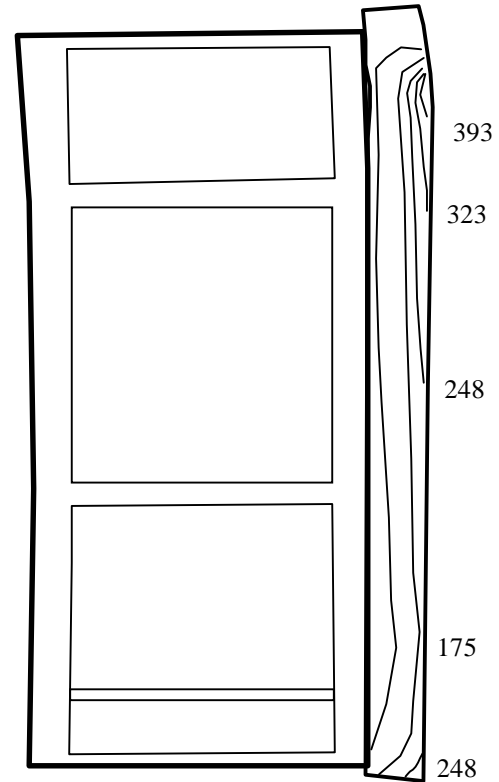


Fig.13 End view of distorted mould along the wide face centerline showing the gap between copper plate and water jacket and temperature profiles

Fig.14 shows the total stress-strain history at the position of 75mm from the meniscus during the first casting heat and subsequent cooling for the parallel mould. When the mould temperature increases from room to operating temperature, the mould tries to expand, but is constrained by the bolts on the water jacket, forcing most of the mould into compression. The highest compressive stress occurs on the hot face of the mould, where the temperatures are highest. Upon cooling, the mould tries to contract but is once again restrained from doing so by the bolts in the backing plate. This causes the inner face of the mould to go into tension as shown in Fig.14. If over-constraining condition took place around 400mm from the

center of mould width, such as caused by large pretension of tightening bolt and high temperature, these stresses may increase the high possibility of mould crack occurrence.

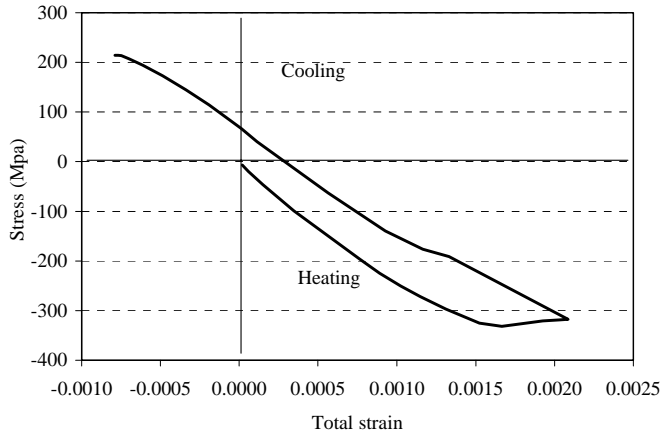


Fig.14 Stress-strain hysteresis loops on the hot face of parallel mould

Fig.15 shows the evolution of thermal distortion on vertical section for the parallel mould during the first heat and subsequent cooling, whose behavior is similar to conventional slab mould [1].

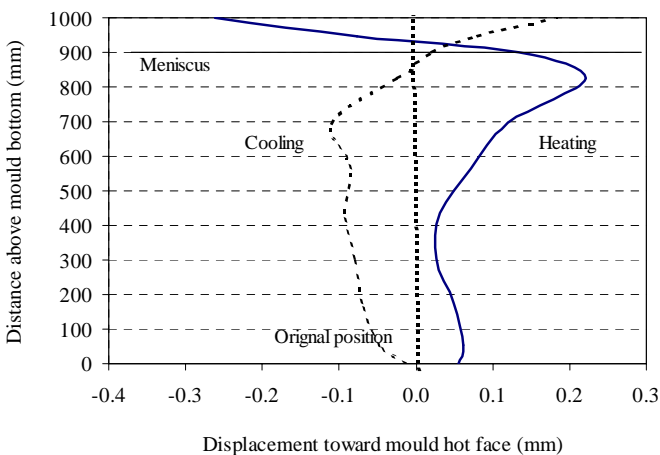


Fig.15 Predicted evolution of thermal distortion on vertical section for the parallel mould

Fig.16 shows the evolution of thermal deflection of the wide face during operation for given hot-face temperature profile according to the mould shape and the mould position. In the case of the mould temperature field, the pseudo-mould model of both the parallel and funnel mould has almost same temperature profile as shown in Fig.16 (a). As can be seen from Fig.16 (b), the deflection behavior for the parallel mould does not change much with position across the mould width. However, the funnel mould deflection varies considerably with position. Specifically, the center of the mould width corresponding to the funnel region has less deflection while the edge region of the funnel has more deflection, relative to the parallel mold

Fig.17 shows the same behavior of the hot face across the mould width at the 75mm position below the meniscus. In the parallel mould the deflection is constant across the slab width. On the other hand, the deflection increases across the mould width in the funnel mould.

Fig.18 shows the deflection of backing plate relative to the original position along the wide face. Distortion of the funnel mould is larger than that of the parallel mould.

When casting a slab, gaps form near the narrow face of mould because of shrinkage of the solidifying shell in the wide face. Therefore, the size of the gap between the shell and mould is controlled by imposing the taper on the mould walls. In order to define the mould taper, in addition to the shrinkage, it is also important to know how the mould deforms because deformation contributes to the mould taper.

Fig.19 shows the displacement of the narrow face of the mould, which is similar to the wide face. This deformation behavior is affected by the wide face and backing plate. The narrow face is connected to the wide face only through clamping

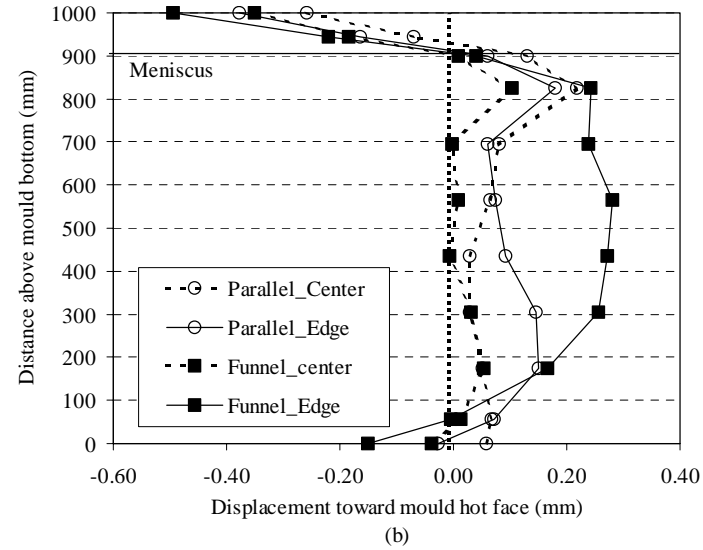
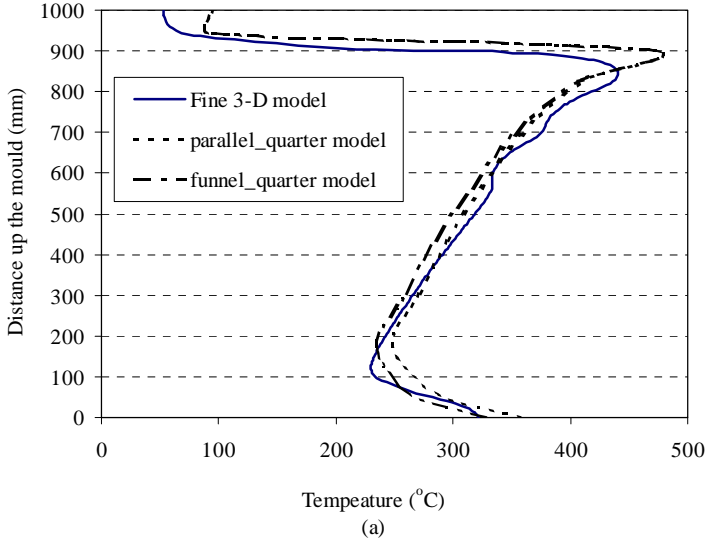


Fig.15 Predicted evolution of thermal distortion on the vertical section (b) with corresponding hot face temperature profiles (a) according to the mould shape and mould positions

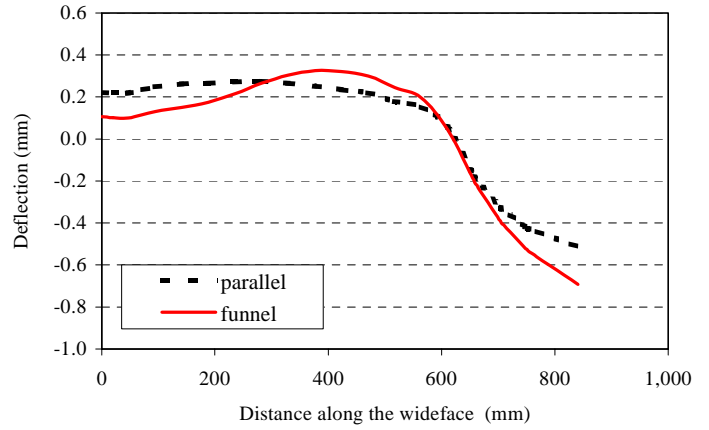


Fig.17 The behavior of mould distortion during operation along the wideface just below the meniscus

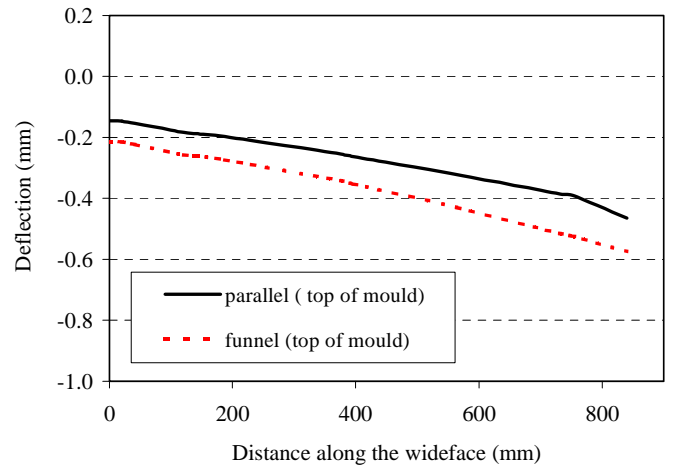


Fig.18 The behavior of back plate distortion during operation according to the mould shape

pressure, and the wide face is free to rotate around the expanded narrow face, contacting only along a small portion of the front vertical edge of the narrow face. As the wide face rotates outward, away from its original position as in the case of funnel mould, the reaction force on the narrow face becomes smaller. Consequently, the deformation is smaller for the narrow face of the funnel mould as shown in Fig.19.

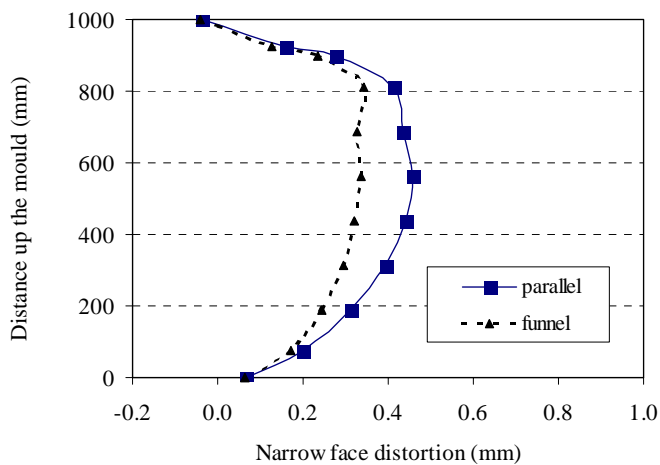


Fig.19 Predicted profiles of narrow face distortion with the mould length

## 6. CONCLUSION

1. Heat fluxes were calculated for operational thin slab casters based on the measured mould temperature, and heat flux profiles were fitted to the calculated heat flux values.

2. A 3-D thermal-elastic-plastic-creep model has been developed to predict the behavior of thermal and mechanical behavior of thin slab mould using ABAQUS. And the model predictions of temperature and distortion during operation match plant observations. During

operation, the hot face temperature reaches 430°C and the copper plates bend toward the steel, with a maximum outward distortion of about 0.3mm. This occurs just above the center of the wide faces, and is not larger than the distortion of a conventional mould.

## ACKNOWLEDGEMENTS

The authors would like to thank POSCO for permission to publish this paper. In addition, special thanks are extended to S.Y.Kim, O.D.Kweon, W.W.Hur, and C.H.Yim for their cooperation and assistance.

## REFERENCE

1. B.G. Thomas, G.Li, A.Moitra and D.Habing, "Analysis of Thermal and Mechanical Behavior of Copper Moulds During Continuous Casting of Steel Slabs", Iron and Steelmaker, Oct, 1998, pp.125-143.
2. Huang, B.G.Thomas, and F.M.Najjar, "Modeling Superheat Removal During Continuous Casting of Steel Slab, 1988 Steelmaking Conference Proceeding, Vol.71, 1988, pp.411-421.
3. D.M.Salkiewicz, J.O.Ratka, "Development and Performance Results-High Performance Copper Alloy for Continuous Casting Moulds", 1995 Steelmaking Conference Proceeding, Vol.78, 1995, pp.369-376.
4. Thomas G.O'Connor and Jonathan A.Dantzig, "Modeling the Thin-Slab Continuous -Casting Mould", Metallurgical and Materials Transaction B, Vol.25B, 1994, pp.443-457.

5. C.A.M. Pinheiro, "Mould Thermal Response, Billet Surface Quality and Mould Flux Behavior in the Continuous Casting of Steel Billets with Powder Lubrication", Ph.D Thesis, 1997, University of British Columbia, Vancouver, Canada.
6. D.P. Evteev, "Fundamental Laws of Heat Exchange Between Continuous Casting Mould and Slab", Stal in English, Vol.20, 1969, pp.708-711.
7. E.A. Upton, T.R.Satya Rao, P.H.Dauby and R.C. Knechtges, "Physical Metallurgy and Mathematical Modelling as Tools for Continuous Casting Optimization at KTV Steel", Iron and Steelmaker, Vol. 15, No.5, 1988, pp.51-57.
8. R.Davies, N.Blake and P.Campbell, "Solidification Modelling-An Aid to Continuous Casting", Proceedings of the 4th International Conference on Continuous Casting, Brussels, Belgium, Vol.2, 1988, pp.645-654.
9. J.Konishi, "Modelling of the Formation of Longitudinal Facial Cracks in the Continuous Casting of Steel Slabs", M.A.Sc. Thesis, 1996, University of British Columbia, Vancouver, Canada.
10. S.Hiraki, K. Nakajima, T.Murakami and T.Kanazawa, "Influence of Mould Heat Fluxes on Longitudinal Surface Cracks during High Speed Continuous Casting of Steel Slab", 77th Steelmaking Conference Proceedings, ISS-AIME , 1994, pp.397-403.
11. R.B.Mahapatra, J.K.Brimacombe and I.V.Samarasekera , "Mould Behavior and Its Influence on Quality in the Continuous Casting of Steel Slabs: Part II. Mould Heat Transfer, Mould Flux Behavior, Formation of Oscillation Marks, Longitudinal Off-Corner Depression, and Subsurface Cracks:", Met. Trans. B, Vol. 22B, 1991, pp.875-888.
12. M.M. Wolf, "Mould Heat Transfer and Lubrication Control-Two Major Functions of Caster Productivity and Quality Assurance", 13th Process Technology Division Conference Proceedings, ISS-AIME, 1995, pp.99-117.
13. K.Hibbit and J.Sorensen, ABAQUS, Providence, RI, 1996.
14. J.Szekely and N.J.Themelis, "Reate Phenomena in Process Metallurgy", Wiley-Interscience, New York, 1971.
15. O.D.Kweon, POSCO, Pohang, Korea, Personal Communication.
16. G.Carlsson, B.Brolund and R.Nystrom, "Measurement of Mould Distortion and Mould Heat Flux in Industrial Caster", Journes Siderurgiques ATS, Paris, Dec.6-7, 1989.
17. M.R.Ozgu, "Continuous Caster Instrumentation: State-Of-The-Art Review", Can.Met.Quart., Vol.35, No.3, 1996, pp.199-223.
18. Technical Information 0805, KM Europa Metal, AG.